Anomalies in the structural and electrical properties of the amorphous semiconductor a-GaSb:Ge

V. V. Brazhkin, A. G. Lyapin, and S. V. Popova

Institute of High Pressure Physics, Russian Academy of Sciences, 142092 Troitsk, Moscow Oblast.

S. V. Demishev, Yu. V. Kosichkin, D. G. Lunts, N. E. Sluchanko, and S. V. Frolov

Institute of General Physics, Russian Academy of Sciences, 117942 Moscow

The effect of a germanium dopant in gallium antimonide on the structure and properties of bulk amorphous samples has been studied. The samples were synthesized by solid-phase amorphization at high pressure. The structure of the a-GaSb:Ge samples, the crystallization temperature and activation energy, and the heat of crystallization have been determined. As the germanium concentration is increased to $x_{Ge} = x_{Ge}^* \approx 27$ mole %, the phase composition of the samples changes sharply. At $x_{Ge} < x_{Ge}^*$ there is a mixture of phases, including crystalline GaSb and Ge in addition to the tetrahedral amorphous phase. At $x_{Ge} > x_{Ge}^*$ the samples are a homogeneous disordered tetrahedral a-GaSb:Ge network. Upon heating, the amorphous phase a-GaSb:Ge crystallizes into a metastable solid solution $(GaSb)_{1-x}Ge_x$. A doping level $x_{Ge} \leqslant 43$ mole % results in an increase in the radius of the first coordination sphere of the a-GaSb:Ge amorphous alloys, in contrast with the decrease in the mean shortest interatomic distance in crystalline alloys of the corresponding composition. In addition to the change in phase composition, the doping results in a substantial modification of the characteristics of the a-GaSb amorphous phase. Doping with germanium makes it possible to vary the resistivity of the system by a factor of $\sim 10^9$ at $T \sim 100$ K. It also makes it possible to vary the characteristics of the samples from those of a metastable amorphous superconductor to an amorphous insulator. A joint analysis of data on the temperature dependence of the conductivity and that of the thermoelectric power shows that the current and energy transport in the a-GaSb system is anomalous. It cannot be described satisfactorily by the existing theories for multicomponent media, even when the possibility of a polaron transport is also taken into account. A change in the conductivity type of a-GaSb:Ge samples as a result of doping has been observed. The superconductivity of a-GaSb:Ge can be explained in terms of the presence of a nonstoichiometric $Ga_y Sb_{1-y}$ amorphous phase. The data obtained on the critical field $H_{c2}(T)$ show that the observed features of the superconductivity arise from a substantial difference between the characteristics of $Ga_y Sb_{1-y}$ inclusions with $y > 0.8$ and $y < 0.8$. A model relating the structural anomalies of the a:GaSb:Ge samples with a relaxation of local stressed regions which arise during synthesis under pressure is proposed.

1. INTRODUCTION

The doping of amorphous semiconductors remains a leading problem in the physics of the noncrystalline state.[1-5] In addition to the obvious practical applications of this field of research, which arise from the problem of controlling the properties of an amorphous material, there is the fundamental aspect associated with the introduction of impurity atoms in a disordered matrix. Since the concentration of intrinsic defects in amorphous semiconductors is much higher than that in their crystalline analogs, the effect of a dopant can be significant at concentrations above those which are ordinarily used (and which are sufficient) to control the properties of crystalline semiconductors.

In this situation the dopant may not only alter the properties of the amorphous network as it becomes incorporated in the latter, but can also lead to the formation of inclusions of phases different from the original material. It is the latter mechanism which is responsible for the doping of glassy chalcogenide semiconductors,[4] which were regarded for a long time as not amenable to doping.[1,2] The doping problem has been studied in most detail for the case of amorphous silicon and related materials.[1] For that class of amorphous semiconductors, it has now been established that it is possible to change the conductivity type and to vary the carrier density over a wide range.[5] In addition, a fundamental understanding of the doping mechanisms has been reached in that case.[1,5]

Recent progress in methods of solid-phase amorphization has made it possible to study a new class of amorphous semiconductors, those synthesized at high pressure.[3,6,7] The problem of doping these semiconductors was originally raised in Ref. 3, where a study was made of the changes effected by a copper dopant in the properties of a-GaSb synthesized under pressure. It was found that at concentrations $x_{Cu} \sim 10$ mole % a solubility limit of copper
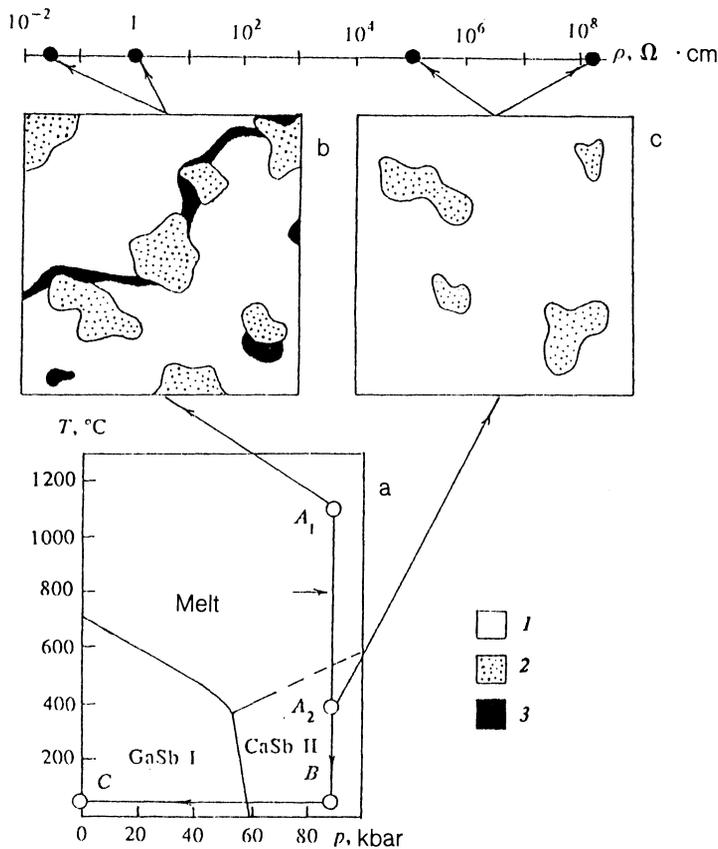
FIG. 1. a: Method for synthesizing the metallic and insulating samples of a-GaSb:Ge. b, c: Schematic diagram of the structure of these samples at $x_{Ge}=0$, for the metal and insulator, respectively. 1—a-GaSb; 2—c-GaSb; 3—$Ga_y Sb_{1-y}$. Shown for comparison is a scale of the resistivity of the a-GaSb samples at $T=4.2$ K according to the data of Refs. 3 and 6.

in the amorphous matrix of gallium antimonide was reached, and inclusions of a crystalline phase of the intermetallic compound $Ga_4 Cu_9$ formed.[3] This effect seriously hindered the efforts to analyze the changes in the characteristics of the a-GaSb amorphous phase proper.

Our purpose in the present study was to learn about the effect of a dopant on the physical properties of the amorphous matrices of amorphous semiconductors synthesized under high pressure. As the test samples we selected bulk samples of amorphous gallium antimonide, for which the synthesis procedure has been refined to the greatest extent.[3,6] As the dopant we selected the group-IV element germanium.

There were several motivations for this choice. A Ge dopant in a III–V semiconductor is amphoteric,[8] and its type of electrical activity depends on which atom is replaced. In the case of III–V compounds containing gallium, particularly GaSb, germanium usually replaces gallium and leads to an n-type conductivity. One can thus use the changes in the conductivity type of the system to draw conclusions about the microscopic mechanisms of the structural changes in a-GaSb:Ge samples. In addition, there is the possibility of producing n-type samples of amorphous semiconductors synthesized under pressure in this system. All the amorphous semiconductors synthesized under pressure which have been studied to date have exhibited exclusively a p-type conductivity,[3,6,9] so their potential practical applications have been seriously limited.

It also follows from data in the literature[10] that synthesis under pressure can substantially increase the solu-

bility limit of the dopant.[7,10] In the case of GaSb, this effect should be expected in the case of specifically a germanium dopant, since in this case metastable crystalline solid solutions $(GaSb)_x Ge_{1-x}$ can form over the entire interval $0 \leqslant x \leqslant 1$. In contrast, the equilibrium solubility of germanium in gallium antimonide is no greater than a fraction of a mole % (Ref. 10).

The effect of a dopant on the properties of a III–V amorphous semiconductor is of interest in its own right, since there has been essentially no study of this case, to the best of our knowledge.

2. EXPERIMENTAL PROCEDURE AND METHOD FOR SYNTHESIZING THE SAMPLES

Since the structure and other properties of a-GaSb samples depend strongly on the synthesis conditions, we need to discuss the procedure for synthesizing the amorphous gallium antimonide before we take up the effect of the germanium dopant[3,6] (Fig. 1).

The following procedure was used to synthesize the amorphous semiconductor a-GaSb under pressure (Fig. 1a). An original sample of stoichiometric composition was subjected simultaneously to a high pressure $p_{syn} \sim 90$ kbar and a temperature T_{syn} (points A_1 and A_2 on the phase diagram). For amorphization it is important that the pressure p_{syn} exceed the pressure of the GaSbI $\rightarrow$ GaSbII phase transition (Refs. 3, 6, 7). The sample was then quenched to room temperature at $p_{syn} = $const (Fig. 1a; point B in the

phase diagram). The pressure was then withdrawn, and an amorphous bulk sample of a-GaSb was obtained (Fig. 1a, point C).[3,6]

It was shown in Ref. 6 that during amorphization by the $A \to B \to C$ scheme the synthesis temperature T_{syn} is a parameter which has an important effect on the properties of the a-GaSb samples. At $T_{syn} < T^*_{syn} = 800\ °C$, the a-GaSb samples contain residual inclusions of the crystalline phase GaSbI (c-GaSb) along with the tetrahedral amorphous phase. The bulk fraction of these inclusions is 5–7%, and no percolation through the crystallization phase occurs. As a result, the transport properties of the system are determined by the characteristics of the high-resistivity amorphous a-GaSb matrix, and the resistivity of the samples at liquid-helium temperatures reaches $\rho \sim 10^8\ \Omega \cdot cm$ (Ref. 6).

The structure of the system and nature of its conductivity change substantially at $T_{syn} > T^*_{syn}$. In the first place, the volume fraction of the crystalline phase increases to ~ 10–15%. In addition, inclusions of a nonstoichiometric amorphous $Ga_y Sb_{1-y}$ phase arise in the interior of the sample.[6] For $y > 0.5$ these inclusions exhibit a superconductivity with a transition temperature in the interval $1.8 \leqslant T_c \leqslant 10$ K, depending on the particular composition.[6,11] The volume fraction of the $Ga_y Sb_{1-y}$ inclusions does not exceed 3–5% (Refs. 3 and 6). Nevertheless, they and the crystalline inclusions form a subnetwork of low-resistivity conducting channels which shunt the high-resistivity amorphous matrix. As a result, the conductivity of the system increases sharply, and the resistivity at $T \sim 10$ K becomes $\rho \sim (2 \cdot 10^{-2} - 1)\ \Omega \cdot cm$ (Ref. 6).

Figure 1, b and c, shows a schematic diagram of the structure of the a-GaSb samples for $T_{syn} > T^*_{syn}$ and $T_{syn} < T^*_{syn}$, respectively, according to x-ray diffraction and measurements of kinetic properties.[3,6]

The physical reason for the formation of the $Ga_y Sb_{1-y}$ inclusions appears to be a disruption of the congruence of the melting of a-GaSb at $T > T^*_{syn}$. When a molten material containing regions with excess gallium or antimony is quenched, nonstoichiometric inclusions form in the interior of the sample. A reduction of T_{syn} to values $T_{syn} < T^*_{syn}$ prevents the dissociation of the components in the melt, and $Ga_y Sb_{1-y}$ inclusions do not form.[3,6]

The a-GaSb samples synthesized under pressure form thus two large groups, depending on the synthesis conditions: "metallic" samples ($T_{syn} > 800\ °C$; Fig. 1b) and "insulating" ones ($T_{syn} < 800\ °C$; Fig. 1c). In the present study we investigated the effect of a germanium dopant on the properties of both metallic and insulating a-GaSb samples over a broad range of germanium concentrations $x_{Ge} \leqslant 50$ mole %. As the original samples we used specially synthesized alloys of c-GaSb and crystalline germanium in which the typical size of the germanium inclusions was ~ 1 μm. A special effort was made to monitor the homogeneity of the germanium distribution in the GaSb:Ge alloy. To synthesize metallic a-GaSb:Ge samples we used an $A_1 \to B \to C$ scheme with $T_{syn} = 1100\ °C$; the insulating samples were synthesized by an $A_2 \to B \to C$ scheme with $T_{syn} = 400\ °C$ (Fig. 1a; $p_{syn} = 90$ kbar).

The procedure for studying the galvanomagnetic and thermoelectric effects is described in detail in Refs. 3 and 6. The structure of the samples was studied by x-ray diffraction with a Dron-2 diffractometer. To determine the activation energy and the heat of crystallization by differential thermal analysis, we used a Derivatograph C instrument (manufactured in Hungary).

3. STRUCTURE OF THE a-GaSb:Ge SAMPLES

The normalized structure factors $a(s)$, where $S = 4\pi \sin \theta / \lambda$ is a structure argument,[12] were determined for the metallic and insulating a-GaSb:Ge samples from curves of the intensity of x-ray scattering, $I(s)$, after the necessary corrections were made and the instrumental background subtracted.[12] Figure 2a shows a typical result for the function $a(s)$.

It was found that in the germanium concentration range $x_{Ge} < 23$ mole % there are some crystal lines (the dashed lines in Fig. 2a) in addition to the oscillatory $a(s)$ curve typical of the tetrahedral amorphous phase a-GaSb. The most intense lines (set 1) correspond to the c-GaSb phase, while line 2 corresponds to crystalline germanium c-Ge. Line 2 in Fig. 2a is not unique, but for values of the structure argument $s \leqslant 4\ Å^{-1}$ the c-Ge lines fall in a region in which the function $a(s)$ varies sharply. In the interval $s \geqslant 4\ Å^{-1}$, the signal-to-noise ratio is degraded. As a result, line 2, which falls near the second amorphous peak in $a(s)$, was used to detect the presence of small amounts of a c-Ge impurity in the samples.

As the germanium concentration is raised, the relative height of the c-GaSb crystal line, I_c/I_0 ($I_0 = I_c + I_a$, where I_a is the height of the first amorphous peak), initially increases slightly for the first peak in the function $a(s)$. At a higher concentration, $x_{Ge} > 8$ mole %, this relative height begins to decrease; it vanishes at $x_{Ge} \sim 23$ mole % (see the inset in Fig. 2a). A further increase in the germanium concentration does not give rise to any crystal lines, and the function $a(s)$ takes the form shown by the solid line in Fig. 2a. The samples remain homogeneous and amorphous up to $x_{Ge} \sim 80$ mole%.

Similar changes apparently occur in the relative amplitude of the I_c/I_0 line for c-Ge (line 2). For this structural feature, however, the error in the determination of this parameter was much larger, up to ~ 50–70%. A study of the metallic samples ($T_{syn} = 1100\ °C$) and the insulating ones ($T_{syn} = 400\ °C$) revealed no systematic differences in the behavior of the function $a(s)$, except a slightly greater height I_c for c-GaSb in the metallic samples at $x_{Ge} = 0$. The latter feature agrees with the results of previous[6] structural studies of a-GaSb.

With increasing x_{Ge} the a-GaSb samples thus evolve from the complex polyphase structure shown schematically in Fig. 1 into a spatially homogeneous disordered a-GaSb:Ge network. The situation here is quite different from that in the case of doping with copper, since for a-GaSb:Cu samples there is a copper solubility limit in the amorphous matrix.[3] In the case of a germanium dopant the situation is just the opposite: the system becomes more
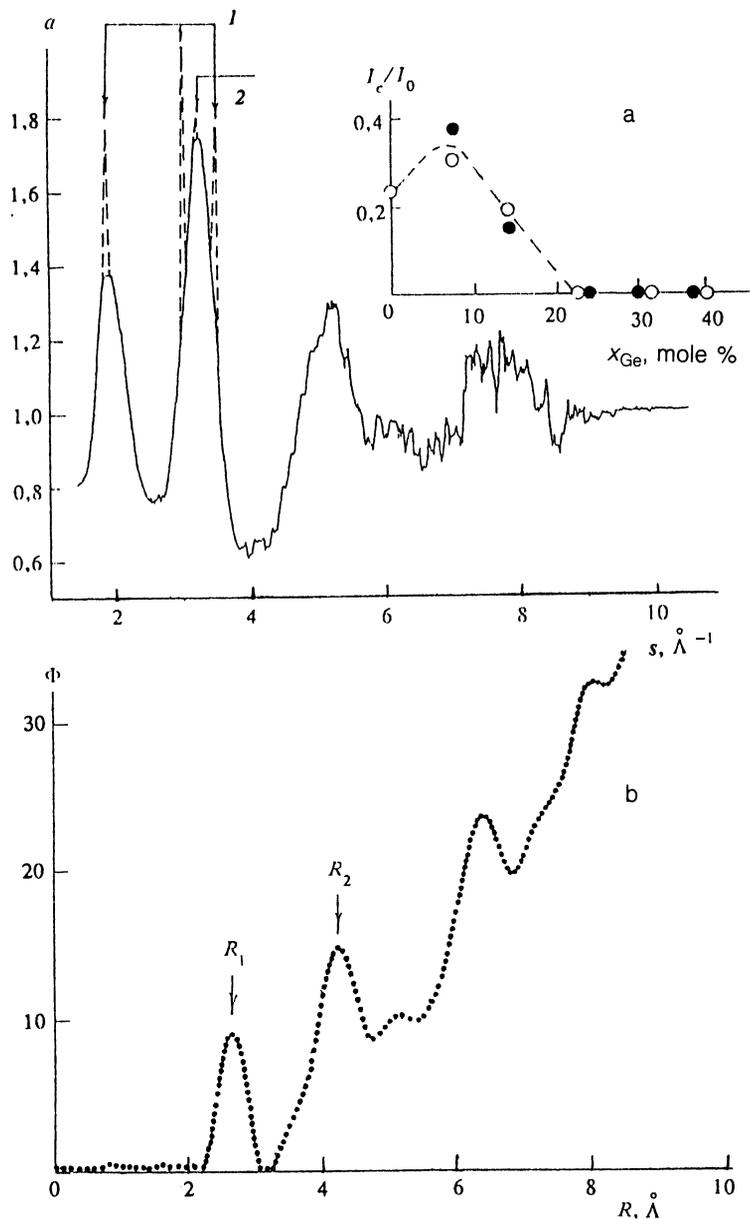
FIG. 2. a: Structure factor. b: Radial profile for a sample with $x_{Ge}=36.7$ mole % ($T_{syn}=400$ °C). The dashed lines are "crystal" lines for $x_{Ge}=14.4$ mole %. 1—c-GaSb; 2—c-Ge. The inset shows the behavior of the relative amplitude of the crystal lines as a result of the doping, for metallic samples (filled circles) and insulating samples (open circles).

nearly homogeneous as x_{Ge} increases. This behavior persists up to at least $x_{Ge} \sim 80$ mole %.

In addition to the changes in the structure of the a-GaSb samples, we observe a change in the shape of $a(s)$ curves. To analyze these changes, we worked from the $a(s)$ curves to calculate the correlation length $L_c(x_{Ge})$ (Ref. 13) and the radial profile

$$\Phi(R)=4\pi R^2 \rho_a(R),$$

where $\rho_a(R)$ is the atomic density. The procedure used to calculate $\Phi(R)$ was the standard procedure, the same as that described in Ref. 12. Figure 2b shows a representative radial profile for the structure factor $a(s)$ in Fig. 2a. The data on the first and second coordination spheres [the first and second peaks in $\Phi(R)$] are the most reliable. As a result, we found the concentration dependence of the radii of the first and second coordination spheres, R_1 and R_2 [the positions of the first and second peaks in $\Phi(R)$], and also

the concentration dependence of the corresponding coordination numbers n_1 and n_2 [the area under the first and second peaks in $\Phi(R)$].

For a-GaSb:Ge samples with $x_{Ge} < 50$ mole %, the coordination number $n_1 \approx 4$ and the radius of the second coordination sphere, $R_2 \approx 4.22 \pm 0.01$ Å, are essentially independent of the germanium concentration. The value $n_1 \approx 4$ corresponds to tetrahedral bonds in the amorphous a-GaSb:Ge network. The parameters R_1, n_2, and L_c, on the other hand, depend strongly on the doping level (Fig. 3). The radius of the first coordination sphere, R_1, increases with x_{Ge}, from $R_1=2.61 \pm 0.01$ Å ($x_{Ge}=0$) to $R_1=2.65 \pm 0.01$ ($x_{Ge} \sim 42$ mole %) (Fig. 3a). At the same time (Fig. 3b), the ratio n_2/n_1 changes from $n_2/n_1 \approx 2.7$ to $n_2/n_1 \approx 3$ (the latter value is characteristic of an ideal ordered tetrahedral network which contains no defects, and for which we would have $n_1=4$ and $n_2=12$). In this concentration range the correlation length L_c decreases by
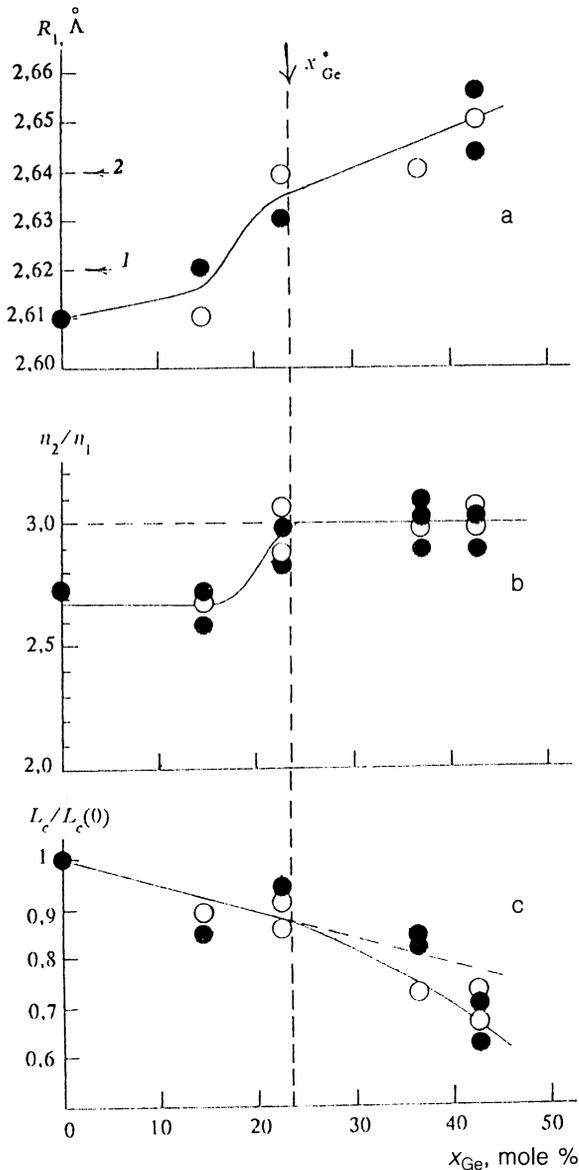
FIG. 3. Concentration dependence of structural properties. Open circles—insulating samples ($T_{syn}=400$ °C); filled circles—metallic samples ($T_{syn}=1100$ °C).

no systematic differences between the insulating and metallic samples.

The increase in $R_1(x_{Ge})$ in the concentration range studied, $x_{Ge} \leqslant 43$ mole %, is anomalous. It cannot be explained by the standard arguments regarding the doping of semiconductors. The covalent radii for the Ga, Sb, and Ge atoms are $R_c^{Ga} = 1.26$ Å, $R_c^{Sb} = 1.36$ Å, and $R_c^{Ge} = 1.22$ Å, respectively.[8,14,15] Since the inequalities $R_c^{Ge} < R_c^{Ga}, R_c^{Sb}$ hold for a-GaSb:Ge system, the interatomic distances should decrease on the average when germanium is added. This is indeed what is observed in familiar semiconductors when a dopant with a smaller covalent radius is added.[15] On the other hand, the experiments show that the value of $R_1(x_{Ge})$ of a-GaSb:Ge does not decrease; it in fact increases (Fig. 3a).

Note also that the value of R_1 in the region $x_{Ge} < 15$ mole % is approximately equal to half the sum of covalent radii $R_c^{Ga} + R_c^{Sb} = 2.62$ Å (Fig. 3). This approximation of the bond length turns out to be rather crude in the case c-GaSb. For the gallium antimonide crystal we have $R_1 = a\sqrt{3}/4 = 2.64$ Å, where $a = 6.096$ Å is the length of a side of the elementary cube.[16] Amorphous gallium antimonide samples are thus denser than the unstressed defect-free crystal network.

These results suggest the following mechanism for the anomalous change in the structure of a-GaSb samples with increasing germanium concentration. The original ($x_{Ge}=0$) a-GaSb samples contain a fair number of locally stressed regions in which the bond length is smaller than the equilibrium value. As a result, the inequality

$$R_1 \sim R_c^{Ga} + R_c^{Sb} < a\sqrt{3}/4$$

holds. We might expect that these structural deviations would be associated with boundary regions between amorphous and crystalline phases, which are characterized by sharp changes in the order parameter and in which the residual stress is most likely to be concentrated. We might note that it is in the boundary region that the metallic phase $Ga_y Sb_{1-y}$ is found in the case of metallic samples.[3,6]

The addition of germanium apparently leads to an effective stress relaxation in the amorphous GaSb network. As a result, R_1 increases to values close to the equilibrium value $R_1 \sim a\sqrt{3}/4$. This change in structure is accompanied by a redistribution of atomic density between the first and second coordination spheres (a change in the ratio n_1/n_2). At the same time, the stress relaxation in the amorphous network leads to an "added amorphization" of the inclusions of the crystalline phase. An additional disordering of the amorphous structure of this sort has been observed previously[17] in Cu–Sn and Cu–Al alloys subjected to mechanical effects.

The structures of the a-GaSb:Ge samples at $x_{Ge} < x_{Ge}^*$ and $x_{Ge} > x_{Ge}^*$ are thus quite different. The range $x_{Ge} < x_{Ge}^*$ is characterized by a highly stressed tetrahedral amorphous network, in which the bond lengths are substantially distorted. At $x_{Ge} > x_{Ge}^*$, a significant fraction of the "built-in" local stress has relaxed, and the tetrahedral amorphous network has become "more nearly perfect" as a

$\sim 30\%$, and we have $L_c(x_{Ge}=0) \sim 20$ Å, in agreement with data found previously.[6]

The typical germanium concentration $X_{Ge}^* \approx 23$ mole % which we introduced above as the boundary separating the region of polyphase samples from the region of single-phase samples (Fig. 2) correlates with structural features on the $R_1(x_{Ge})$, $n_2(x_{Ge})$, and $L_c(x_{Ge})$ curves (Fig. 3). In the region 15 mole % $< x_{Ge} < x_{Ge}^*$ we see a region of a sharp growth of $R_1(x_{Ge})$ and $n_2(x_{Ge})$, while at $x_{Ge} > x_{Ge}^*$ the $R_1(x_{Ge})$ curve shows a tendency toward saturation, while the ratio n_2/n_1 approaches a steady-state $n_2/n_1=3$ (Fig. 3, a and b). In the case of the correlation length at $x_{Ge} > x_{Ge}^*$ there is an increase of the slope of $L_c(x_{Ge})$ curve in comparison with that in the region $x_{Ge} < x_{Ge}^*$ (Fig. 3c). According to the data in Fig. 3, there are
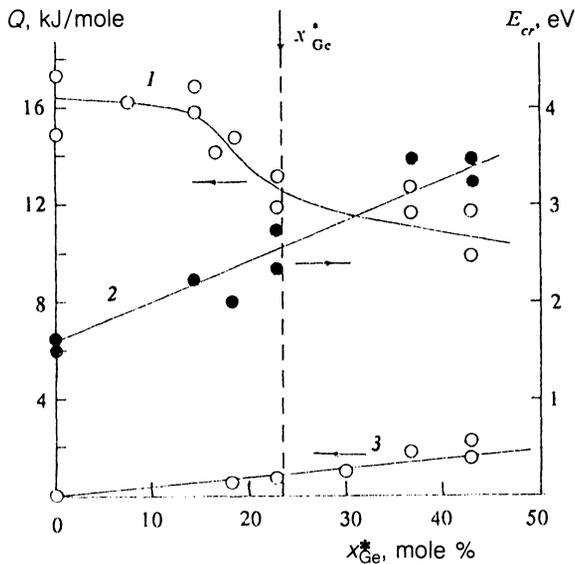
FIG. 4. Heat of crystallization (1) and activation energy for crystallization (2) for a-GaSb samples. 3—Data on $Q'(x_{Ge})$ for the metastable solution $(GaSb)_{1-x}Ge_x$.

result. Interestingly, the correlation length decreases in the process, and the stress relaxation leads to an addition disordering in the a-GaSb:Ge system.

Further evidence in favor of this model comes from the concentration dependence of the heat of crystallization, Q, and the crystallization activation energy E_{cr} (Fig. 4). An energy associated with disordering, including energy stored in the form of various local stresses in the amorphous phase, evidently is released in the course of crystallization. A decrease in the volume fraction of stressed regions should lead to a decrease in Q, and this is what we see experimentally: $Q(x_{Ge})$ decreases with increasing x_{Ge} (curve 1 in Fig. 4).

This is not the only cause of a decrease in Q. A special structural study revealed that a metastable solid solution $(GaSb)_{1-x}Ge_x$ forms when a-GaSb:Ge is crystallized in the region $180 \leqslant T \leqslant 390$ °C, which is the region of the main peak in the heat evolution.[10] Since the thermodynamic potential of a metastable solid solution is higher than the thermodynamic potential of c-GaSb, its increase in x_{Ge} may lead to a decrease in Q.

To study this question we measured the heat Q' which corresponds to the decomposition of $(GaSb)_{1-x}Ge_x$ at $T \geqslant 400$ °C (curve 3 in Fig. 4). We see that Q' increases linearly with x_{Ge}, but it is lower, over the entire studied concentration range $x_{Ge} \leqslant 50$ mole %, than the amplitude of the change in Q in the interval $x_{Ge} \leqslant 43$ mole % (curve 1 in Fig. 4). The predominant cause of the decrease in the heat of crystallization of the tetrahedral amorphous phase in a-GaSb:Ge samples is thus apparently a relaxation of local stress due to the doping with germanium. A stress relaxation in an amorphous network should also lead to an increase in the stability of the amorphous structure. As a result, the height of the barrier in configuration space which separates stable and metastable states increases.
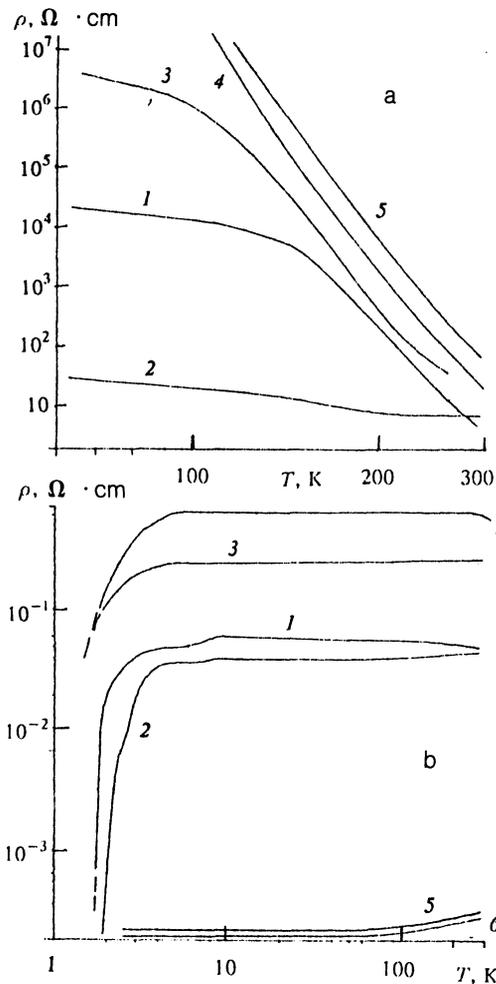

FIG. 5. Temperature dependence of the resistivity in the a-GaSb:Ge system. a) Insulating samples ($T_{syn} = 400$ °C) 1—$x_{Ge} = 0$; 2—7.5 mole %; 3—19; 4—23; 5—37 mole %. b) Metallic samples ($T_{syn} = 1100$ °C) 1—$x_{Ge} = 0$; 2—7.5 mole %; 3—14; 4—19 mole %. Shown for comparison are data on $\rho(T)$ for the original crystalline alloys: 5—$x_{Ge} = 23$ mole %; 6—37 mole %.

Consequently, the crystallization activation energy E_{cr} increases with increasing germanium concentration. Experiments also confirm this conclusion (curve 2 in Fig. 4).

We would naturally expect that the structural transition (in the sense of an evolution of the phase composition) observed here in the disordered semiconductor a-GaSb:Ge would lead to structural features in the kinetic characteristics of this system.

4. ELECTRICAL CONDUCTIVITY OF a-GaSb:Ge SAMPLES; CHANGES IN SUPERCONDUCTING PROPERTIES AS THE RESULT OF DOPING

Figure 5 shows the temperature dependence of the resistivity, $\rho(T)$, for a-GaSb:Ge samples. For insulating samples (Fig. 5a), the behavior is an activation law $\rho = \rho_0 \exp(E_a/k_B T)$ with an activation energy $E_a \sim 200$ meV (curves 3–5 in Fig. 5a). The value of ρ for samples with $x_{Ge} > 19$ mole % is much larger than ρ for the sample with $x_{Ge} = 0$, produced under the same synthesis conditions

($T_{syn} = 400\,°C$; curve 1 in Fig. 5a). The decrease in the resistivity of the samples at $x_{Ge} \sim 7$ mole % in comparison with that at $x_{Ge} = 0$ (curve 2 in Fig. 5a) is attributed to a shunting effect of the c-GaSb and c-Ge crystalline phases, whose relative volume increases slightly in this concentration interval (see the inset in Fig. 2a).

The metallic samples (Fig. 5b) have at $T \geqslant 10$ K a quasimetallic behavior $\rho(T) \approx$ const, with ρ in the interval $2 \cdot 10^{-2} - 1\ \Omega \cdot$ cm. The resistivity of the metallic samples is much lower than that of the insulating ones: At $T \sim 100$ K, the range over which ρ varies as a result of variations in the synthesis conditions and the doping is $2 \cdot 10^{-2} - 10^7\ \Omega \cdot$ cm. In other words, the resistivity changes by a factor of $5 \cdot 10^8$. Shown for comparison in Fig. 5b are data on $\rho(T)$ for the original crystalline alloys c-GaSb+c-Ge (curves 5 and 6). As a result of the disordering of the crystal structure, the resistivity of the a-GaSb:Ge samples increases noticeably.

The concentration dependence $\rho(x_{Ge})$ for the metallic samples at $T \geqslant 10$ K is qualitatively the same as for the insulators: There is a tendency for ρ to increase with x_{Ge}, except in the region $x_{Ge} \sim 7$ mole %. This behavior persists up to $x_{Ge} \sim 20$ mole %. At $x_{Ge} \approx x_{Ge}^*$ there is a sharp increase in ρ to $\rho(T \approx 100$ K$) \sim 10^6\ \Omega \cdot$ cm, accompanied by a change in the shape of the $\rho(T)$ curve from a quasimetallic $\rho(T) \approx$ const to an activation law

$$\rho \sim \exp(E_a/k_B T).$$

A possible explanation of this effect will be discussed in the following section of this paper.

At $T \leqslant 10$ K, the metallic a-GaSb:Ge samples ($T_{syn} = 1100\,°C$) exhibit a drawn-out superconducting transition (Fig. 5b). This transition results from the presence of the nonstoichiometric amorphous phase $Ga_y Sb_{1-y}$ in the interior of the sample.[6,18] At $x_{Ge} = 0$, the a-GaSb samples reach a value $\rho = 0$ at $T \sim 1.8$ K; as x_{Ge} is increased, we do not observe a complete resistance transition, and the conductivity remains finite over the entire temperature interval studied. This behavior can be linked in a natural way with a decrease in the volume fraction of the superconducting inclusions as a result of the doping.

It was shown in Refs. 6 and 18 that the superconducting transition of a-GaSb is percolative, because the superconducting inclusions have different transition temperatures T_c. At $T = T_c = T_m$, those superconducting inclusions which have the highest transition temperature go superconducting. As the temperature is lowered, the volume v_s, occupied by the superconducting phase increases, since the inclusions with $T \leqslant T_c \leqslant T_m$ go superconducting. As a result, at $T = T_p$ the volume v_s may reach a critical value corresponding to the percolation threshold, $v_s = v_p$, and the resistivity may vanish. In the case $v_s < v_p$, the value $\rho = 0$ is not reached.[6,18] It has been suggested[6,18] that the physical cause of the dispersion of T_c is a dispersion of the concentration y for the $Ga_y Sb_{1-y}$ inclusions.[11]

To test that hypothesis and also to study the effect of the germanium dopant on the superconductivity of the $Ga_y Sb_{1-y}$ inclusions, we studied the temperature and field dependence of the resistivity, $\rho(H,T)$, at temperatures

$T \leqslant 10$ K in magnetic fields $H \leqslant 60$ kOe. The mobility of the a-GaSb samples is extremely low, $\mu \leqslant 1$ cm^2/(V$\cdot$s), so we can ignore an effect of the standard magnetoresistance mechanisms on the data on $\rho(H,T)$ in comparison with the effect stemming from a disruption of the superconductivity of inclusions.[6]

Figure 6 shows data on $\rho(H,T)$ for a sample with $x_{Ge} = 14$ mole %. The initial increase in $\rho(H)$, due to the disruption of the superconductivity of the inclusions, gives way to an onset of saturation at $H_m = H_{c2}$, where H_{c2} corresponds to the clusters with the highest transition temperature, $T_c = T_m$. For $T \leqslant 4$ K, two regions appear on the $\rho(H)$ curve for $H < H_m$. For $T = 1.9$ K, for example (curve 8 in Fig. 6), the initial region of a rapid increase in ρ gives way to a transition to a weaker dependence at $H = H'_m \sim 10$ kOe, and the superconductivity is completely destroyed at $H = H_m \sim 30$ kOe.

The anomalous $\rho(H,T)$ behavior (Fig. 6) suggests that the $Ga_y Sb_{1-y}$ inclusions are inhomogeneous in terms of superconducting properties and that phase I with $H_{c2} = H_m$ and $T_c = T_m$ is accompanied by a superconducting phase II with $H_{c2} = H'_m < H_m$ and $T_c = T'_m < T_m$. Using the data on $\rho(H,T)$ and the values found above for the parameters H_m and H'_m, we can reconstruct the $H_{c2}(T)$ dependence for the first and second superconducting phases (see the inset in Fig. 6).

Using this procedure for the a-GaSb:Ge samples with various germanium concentrations, and extrapolating the data on $H_{c2}(T)$ to the values $T = 0$ and $H_{c2} = 0$, we found the values of the parameters T_c, $H_{c2}(T = 0)$, and $dH_{c2}/dT(T \to T_c)$. We determined their concentration dependence for phases I and II (Fig. 7). We found that the characteristics of the superconductivity in phases I and II do not vary in the same way when germanium is added.

While the transition temperature decreases with x_{Ge} in phase I, from $T_c \approx 8$ K ($x_{Ge} = 0$) to $T_c \approx 5.5$ K ($x_{Ge} \approx 20$ mole %), in phase II it increases from $T_c \approx 4$ K to 4.8 K as x_{Ge} varies over the same interval (Fig. 7a). The difference between the behavior of phase I and that of phase II can also be seen in the data on $H_{c2}(0) = f(x_{Ge})$. While we have $H_{c2}(0) \approx 18$ kOe = const for phase II, in phase I the maximum critical field decreases by a factor of about 2 in the concentration range studied: from $H_{c2}(0) \approx 80$ kOe at $x_{Ge} = 0$ to $\sim 40–45$ kOe at $x_{Ge} \geqslant 15$ mole % (Fig. 7b).

The parameter which undergoes the greatest change for superconducting phase II is dH_{c2}/dT. It decreases linearly in absolute value by a factor of 3 at concentrations $x_{Ge} < x_{Ge}^*$. For phase I, the $dH_{c2}/dT = f(x_{Ge})$ dependence is more complicated: Initially, at $x_{Ge} \leqslant 10$ mole %, there is a sharp decrease in dH_{c2}/dT, while at $x_{Ge} > 10$ mole % there is a plateau, $dH_{c2}/dT \approx$ const (Fig. 7c).

Several important conclusions follow from Fig. 7. First, the substantially different behavior of the superconductivity characteristics in phases I and II as a function of the concentration confirms that these are indeed two distinct superconducting phases. Second, the fact that T_c, $H_{c2}(0)$, and dH_{c2}/dT, which are determined by characteristics of the energy spectrum of the superconductor, the carrier density, and the mean free path,[19] depend on the
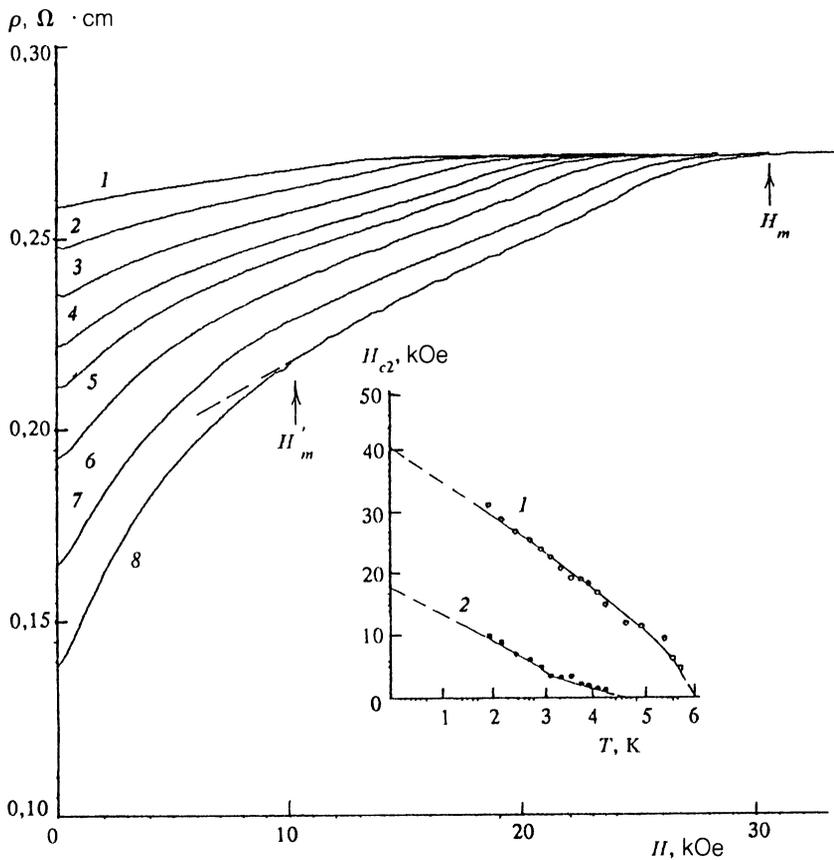
FIG. 6. Disruption of the superconductivity of a metallic sample with $x_{Ge} = 14$ mole % by a magnetic field. The inset shows data on $H_{c2}(T)$ in the field $H_m(1)$ and in the field $H'_m(2)$. The $\rho(H)$ curves correspond to the following temperatures: 1—4.2 K; 2—3.7; 3—3.3; 4—2.9; 5—2.7; 6—2.4; 7—2.2; 8—1.9 K.

concentration indicates that there is a germanium doping of structural phases responsible for the superconductivity of a-GaSb. Third, the superconductivity of the metallic samples persists to the point of the structural transition, $x_{Ge} = x^*_{Ge}$.

We now consider a possible explanation for the anomaly in the superconducting properties of a-GaSb as manifested in the existence of two distinct superconducting phases. We note first that the values $T_c \sim 8$ K and $H_{c2}(0) \sim 80$ kOe in phase I agree with previous results.[6,18] Since these values are approximately the same as those for amorphous gallium, $T_c \approx 8.4$ K and $H_{c2}(0) \sim 100$ kOe (Ref. 20), one might suggest that phase I corresponds to $Ga_y Sb_{1-y}$ with $y \sim 1$. On the other hand, the highest transition temperature of phase II is $T_c \approx 4$ K, and this figure may correspond to a high-pressure GaSb or Sb phase.[21,22] In view of the procedure used to prepare the a-GaSb sample (Fig. 1) and in view of data on the structure of a-GaSb:Ge samples (Sec. 3), we might expect inclusions of these structural phases in locally stressed regions of a sample.

However, this interpretation seems to be refuted by the high values $H_{c2} \sim 17$ kOe in phase II. Data in the literature show that the metastable high-pressure superconducting phases of GaSb and Sb have critical fields H_{c2} no greater than 4–5 kOe (Refs. 21 and 22), much lower than those observed in phase II (Fig. 7).

Let us examine the $T_c(y)$ dependence for the $Ga_y Sb_{1-y}$ phase in more detail. Comparison of the experimental data on $T_c(y)$ found in Ref. 11 with the values found in the

present study (Fig. 7) shows that the composition interval $0.8 \leqslant y \leqslant 1$, for which we have $6.5 \leqslant T_c \leqslant 8$ K, may correspond to phase I, while the range $y \leqslant 0.8$ ($T_c \leqslant 4$ K) may correspond to phase II. Since the value of T_m in phase I is quite different from T_m in phase II, to explain this feature we must assume that $T_c(y)$ decreases abruptly at $y \approx 0.8$ from $T_c \approx 6.5$ to ≈ 4 K as y decreases and that the $T_c(y)$ dependence is as shown by the dashed line in Fig. 7a.

This interpretation—a jump in T_c and H_{c2} between the regions with $y < 0.8$ and $y > 0.8$ in the nonstoichiometric amorphous $Ga_y Sb_{1-y}$ phase—may seem rather arbitrary. However, further arguments can be cited as support. At $y \sim 0.5$ the short-range structure of $Ga_y Sb_{1-y}$ should evidently be approximately the tetrahedral GaSb structure, while at $y \sim 1$ the structure of $Ga_y Sb_{1-y}$ should be approximately that of a typical metal: amorphous gallium. We might expect that the transition between these two types of short-range structure would be a sharp one along the scale of the parameter y. At some $y = y^*$, there would then be a structural transition in $Ga_y Sb_{1-y}$ associated with a change in the short-range structure. This structural transition may be accompanied by a sharp change in the superconducting properties of $Ga_y Sb_{1-y}$. On the basis of the data in Fig. 7 we should assume that the value $y^* \approx 0.8$ corresponds to the transition point. Further evidence in favor of this mechanism comes from the jump observed in Ref. 11 in the conductivity of $Ga_y Sb_{1-y}$ at $y = 0.8$.

We carried out a special study of the effect of annealing on the structure and other properties of metastable phases, in particular, $Ga_y Sb_{1-y}$. This study provided further sup-

T_c, K   1   0,9   0,8   0,7   0,6 y

8

7

6   a

5

4

3

2

100
H_{c2}, kOe

80

60   b

40

20

$-dH_{c2}/dT$, kOe/K

16

12   c

8

4

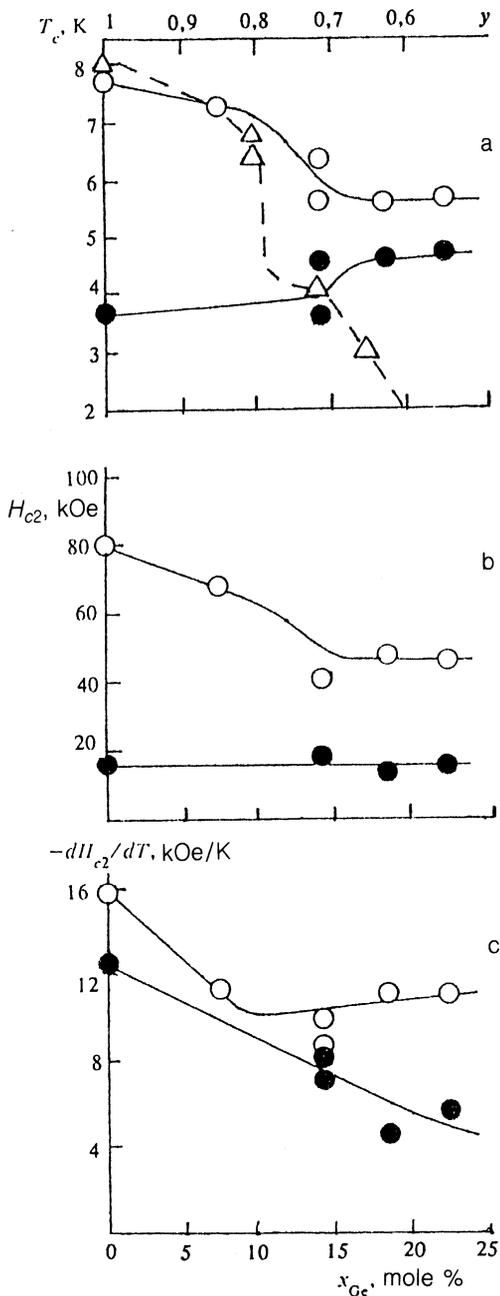0   5   10   15   20   25

x_{Ge}, mole %

FIG. 7. Concentration dependence of superconductivity characteristics of a-GaSb:Ge. Open circles—Phase I ($y > 0.8$); filled circles—phase II ($y < 0.8$). a) $T_c(x_{Ge})$; b) $H_{c2}(0)$; c) $-dH_{c2}/dT(T=T_c)$. The triangles are $T_c(y)$ data from Ref. 11.

port for the interpretation offered above. This question will be the subject of a separate study.

We thus suggest that the anomalies observed in the superconducting properties of a-GaSb can be explained by differences in the structural and other physical characteristics of Ga_ySb_{1-y} at $y < y^*$ and $y > y^*$ ($y^* \approx 0.8$). Phase I corresponds to the region with the highest gallium content, while phase II corresponds to a region with $y < y^*$, in which the short-range structure corresponds to the tetrahedral network of GaSb. The dispersion of the transition temperature can then be explained in a natural way: As y

varies over the interval $1 \geqslant y \geqslant 0.8$ in phase I, the transition temperature T_c varies over the interval $T_m = 8 \geqslant T_c \geqslant 6$ K. In phase II, according to Ref. 11, a reduction of y from $y \sim 0.8$ to $y \sim 0.55$ reduces T_c from $T'_m \approx 4$ K to $T_c \leqslant 1$ K. Since phases I and II are structurally different, the doping with germanium should have different effects on the superconductivity of phases I and II, and this is what is observed experimentally (Fig. 7). Unfortunately, we have so far no data on the critical field of Ga_ySb_{1-y}, so that it is difficult to offer an unambiguous interpretation of the anomalies in the superconducting properties of a-GaSb:Ge. A direct determination of $H_{c2} = f(y)$ for Ga_ySb_{1-y} will be the subject of a further study.

5. FEATURES OF THE CONCENTRATION DEPENDENCE OF THE KINETIC CHARACTERISTICS OF a-GaSb:Ge

The structural transition of a-GaSb:Ge at $x_{Ge} = x_{Ge}^*$ can be seen clearly on the concentration dependence of the kinetic coefficients of the test samples (Fig. 8).

The resistivity of the metallic samples increases abruptly at $x_{Ge} = x_{Ge}^*$, by six orders of magnitude at $T = 100$ K. Thereafter, the conductivities of the metallic and insulating samples are essentially the same (Fig. 8a). The minimum on the $\rho(x_{Ge})$ curves results from the shunting effect of the low-resistivity crystalline phases c-GaSb and c-Ge, as we mentioned above.

The concentration dependence of the thermoelectric power $S(x_{Ge})$ also has a structural feature at $x_{Ge} = x_{Ge}^*$. For the metallic samples (curve 1 in Fig. 8b) there is a jump at the transition point: S increases by a factor of about 100. For the insulating samples (curve 2 in Fig. 8b), the thermoelectric power increases smoothly with x_{Ge}, and the point $x_{Ge} = x_{Ge}^*$ corresponds to an inflection point on the $S(x_{Ge})$ curve. For all the samples studied, the sign of the thermal emf corresponds to a p-type material.

One reason for this behavior of $\rho(x_{Ge})$ and $S(x_{Ge})$ is the disappearance at $x_{Ge} > x_{Ge}^*$ of a subnetwork of conducting channels which is characteristic of metallic samples (Fig. 1). This subnetwork consists of inclusions of c-GaSb, c-Ge, and Ga_ySb_{1-y}. However, it follows from the data in Fig. 8, a and b, that the amplitudes of the jumps in ρ and S at $x_{Ge} = x_{Ge}^*$ are greater than the differences between the values of ρ and S for the metallic and insulating samples at $x_{Ge} = 0$. This indicates that the doping with germanium causes not only a change in the phase composition of the samples but also changes in the kinetic characteristics of the a-GaSb tetrahedral amorphous phase.

Interestingly, while the $\rho(x_{Ge})$ curve for the insulating samples has a minimum at $x_{Ge} \sim 7$ mole %, there is no corresponding feature on the concentration dependence of the thermoelectric power (Fig. 8, a and b). At $x_{Ge} < x_{Ge}^* = 23$ mole % the a-GaSb:Ge samples should be thought of as a polyphase medium. As a first approximation we could consider a two-component medium consisting of a mixture of an "insulator" (the germanium-doped a-GaSb tetrahedral amorphous phase) and a "metal" (inclusions of the crystalline phases c-GaSb and c-Ge). A two-component medium of this sort was examined theoret-
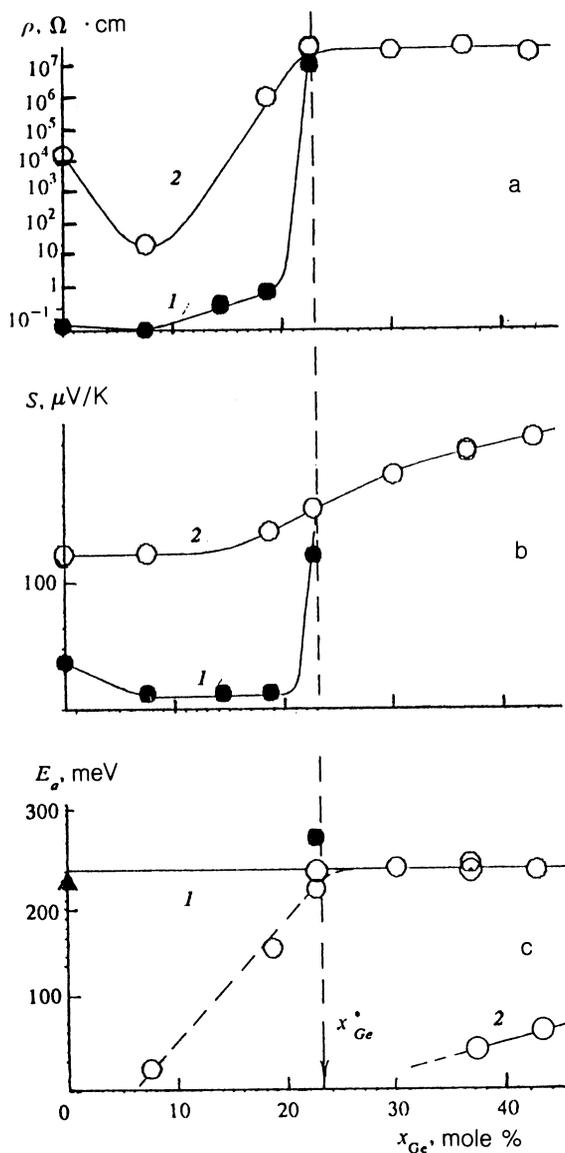
FIG. 8. Concentration dependence of (a) the resistivity at $T=100$ K, (b) the thermoelectric power at $T=300$ K, and (c) the activation energy in the a-GaSb:Ge system. In parts a and b: 1—Metallic samples; 2—insulating. In part c: Open circles—Insulating samples; filled circle—metallic sample. The triangle shows the value of E_a for the conductivity in the case $x_{Ge}=0$. 1) E_a according to the conductivity data; 2) E_a according to the data on the thermoelectric power.

ically in Ref. 23. It was shown that the behavior of the thermoelectric power is determined by the relation between the thermal conductivities of the metal, k_M, and the insulator, k_D.

In the case $k_M \sim k_D$, the critical behavior and thus the concentration dependence of ρ should be qualitatively the

same as those of ρ for the metal.[23] This case was observed experimentally in a-GaSb:Cu (Ref. 3), where the role of the metal was played by inclusions of the intermetallic compound Ga_4Cu_9.

If $k_M \ll k_D$, the thermoelectric power of the two-phase medium is determined by the thermal emf of the insulator up to the threshold for percolation through the metal. In this range of concentrations of the metallic inclusions, the thermoelectric power is independent of the volume fraction of these inclusions.[23] Comparison of the $\rho(x_{Ge})$ and $S(x_{Ge})$ curves (Fig. 8, a and b) shows that this is precisely the case for the a-GaSb:Ge samples. In the case of the insulating samples ($T_{syn}=400$ °C), there is no percolation through the low-resistivity crystalline phases. The shunting effect of these phases is seen in the case of $\rho(x_{Ge})$ but not $S(x_{Ge})$. As a result, the thermoelectric power of the insulating a-GaSb:Ge samples is determined by that of the tetrahedral amorphous phase over the entire range of germanium concentrations studied.

The Hall concentration is another parameter which is sensitive to a germanium dopant in a-GaSb. Unfortunately, the low mobilities and high resistivity of the insulating and metallic samples with $x_{Ge} \approx x_{Ge}^*$ prevented us from obtaining reliable data for this case. The results for the metallic samples ($T=300$ K) are shown in Table I.

Note that the type of conductivity of the metallic a-GaSb:Ge samples changes in the interval $0<x_{Ge}<7.5$ mole %. To the best of our knowledge, this is the first experimental indication of a possible change in the conductivity type of an amorphous semiconductor synthesized at high pressure. This observation opens up some new opportunities for studying materials of this class and for practical applications of them.

There is also a tendency for the Hall mobility μ_H to decrease with x_{Ge} (Table I). This result agrees with the decrease in the correlation length L_c (Fig. 3) with increasing doping level. The parameter L_c, which determines the length scale of the fluctuations in the arrangement of atoms in the disordered network, also determines the length scale of the random potential in which the charge carriers are moving. As L_c decreases, this random potential becomes "choppier," and the scattering intensifies in the system. Another possible cause of a decrease in μ_H would be an increase in the scattering by the short-range potential which arises because of the discrepancy between the covalent radii of the germanium atoms and the atoms making up the tetrahedral network of GaSb.

The Hall concentration n_H (Table I) is a complicated function of x_{Ge}. It appears that the germanium initially compensates for the intrinsic p-type defects which are characteristic of a-GaSb. The germanium should replace pri-

TABLE I. The Hall effect in the a-GaSb:Ge samples.

x_{Ge}, mole %	n_H, 10^{20} cm^{-3}	μ_H, cm^2/(Vis)	Conductivity type according to the Hall effect
0	1,4	0,84	p
7,5	1,2	0,82	n
14	0,52	0,23	n

marily gallium, since in this case it would behave as an n-type impurity.[8] In the case of the metallic a-GaSb samples, this doping mechanism is the most probable one, since in samples containing Ga_ySb_{1-y} inclusions with an excess gallium content we would expect a substantial number of vacancies in the gallium subnetwork of the tetrahedral amorphous or crystalline phase of gallium antimonide. With a further increase in x_{Ge}, the number of gallium vacancies would be exhausted, and there would be the possibility that antimony as well as gallium atoms would be replaced. In this situation we would expect a sort of self-compensation, manifested in a decrease in n_H. This effect apparently agrees with the experimental data (Table I), but a detailed check of the proposed doping mechanism and the determination of the $n_H(x_{Ge})$ behavior constitute a separate problem, outside the scope of the present study.

Comparison of data on the thermal emf and Hall effect of the metallic a-GaSb:Ge samples shows that at $x_{Ge} > 7.5$ mole % there is an anomaly in signs, as is characteristic of many noncrystalline materials.[2] As a rule, however, this effect is observed for insulating samples with an activation-law or hopping conductivity.[2]

In the case of a-GaSb:Ge, the sign anomaly seems to be associated with the polyphase nature of the samples. One might suggest that the conductivity and the Hall effect are determined by low-resistivity inclusions near the threshold for percolation through the metallic phase,[24] while the thermal emf is determined by insulating regions.[25] From this point of view, the change in the Hall concentration results from a change in the type of conductivity of the subnetwork of conducting channels as a result of doping. Here we must assume that a percolation does not occur through the subnetwork of conducting channels at $x_{Ge} > 7.5$ mole %, but the system remains near the threshold for mobility through the metallic phase (c-GaSb, c-Ge, and Ga_ySb_{1-y}). This assumption is supported (Fig. 5) by the decrease in the volume fraction of superconducting inclusions. As a result of this decrease, a percolation through the superconducting regions does not occur at $x_{Ge} \geqslant 7.4$ mole % (Sec. 4). As a result, the shunting effect of the high-conductivity phases is weaker in the case of the thermal emf of the metallic a-GaSb:Ge samples. The effect is probably insufficient to change the sign, although it does reduce the integral value of S for the metallic samples in comparison with that of the insulating samples (Fig. 8b).

It follows from this discussion that the most convenient way to study the effect of a germanium dopant on the kinetic characteristics and conductivity mechanisms of specifically the a-GaSb tetrahedral amorphous phase is to work from the concentration dependence of the thermal emf of the insulating samples. Over the entire range of germanium concentrations studied, this behavior is determined by the thermoelectric power of the amorphous phase and is independent of the shunting effect of the crystalline inclusions. We have accordingly studied the temperature dependence of the Seebeck coefficient of the insulating a-GaSb:Ge samples (Fig. 9).

We found that both at $x_{Ge} < x^*_{Ge}$ and in the interval $x^*_{Ge} < x_{Ge} < 37$ mole % the value of S increases with tem-

perature in the interval $10 \leqslant T \leqslant 300$ K. The $S(T)$ dependence for the metallic sample with $x_{Ge} \approx x^*_{Ge}$ is similar to $S(T)$ for the insulating samples (Fig. 9).

This result calls for a detailed discussion, since the insulating a-GaSb:Ge samples are characterized by an activation-law conductivity. In the case of amorphous semiconductors, such a behavior is usually linked with thermal excitation of carriers from the tail of band states to the mobility threshold, or thermal excitation of carriers out of a band of localized states into the conduction band (or into the valence band).[2,25] In this case the thermal emf would be proportional to the temperature,[2,25]

$$S(T) \propto (k_B/e)E_a/k_BT,$$

and the value of S should increase, not decrease, as the temperature is lowered.

Only at the highest germanium concentrations studied here, $x_{Ge} \geqslant 37$ mole %, do the $S(T)$ curves have a rising region with decreasing temperature (curves 4 and 5 in Fig. 9). A replotting of the data on $S(T)$ at $x_{Ge} \geqslant 37$ mole % in the coordinates $S = f(1/T)$ makes it possible to evaluate the activation energy E_a (see the inset in Fig. 9):

$$E_a(x_{Ge} = 37 \text{ mole } \%) \approx 40 \text{ meV},$$

$$E_a(x_{Ge} = 43 \text{ mole } \%) \approx 60 \text{ meV}.$$

Figure 8c shows data on the activation energy for the conductivity and the thermoelectric power of the a-GaSb:Ge samples. We see that the activation energy for the conductivity in the region $x_{Ge} > x^*_{Ge}$ is more than three times the maximum value of E_a for the thermal emf.

We note also that in the case of the conductivity we have $E_a \approx 220$ meV = const over the entire range of germanium concentrations studied (there are some deviations at 7.5 mole % $\leqslant x_{Ge} < x^*_{Ge}$, which stem from the shunting effect of the impurity crystalline phases and the error in the determination of E_a in this region).

Two alternative models are usually invoked to explain thermoelectric-power anomalies similar to those described above.[25] In the first, the difference between the activation energies for the conductivity and thermoelectric power is due to large-scale fluctuations of the potential.[2] The activation energy for the conductivity should be higher than that for the thermal emf by an amount $\Delta E_a \approx \gamma/6$, where γ is the characteristic distance between the minimum of the conduction band and the maximum of the valence band. It follows from the data in Fig. 8c that we have $\Delta E_a \sim 180$ meV and that for a-GaSb:Ge we should have $\gamma \geqslant 1.08$ eV. This value is more than 0.4 eV greater than the gap width E_g of a-GaSb ($E_g \approx 0.6$ eV at $T = 300$ K in gallium antimonide[26]). Accordingly, that interpretation of the structural features in the thermoelectric power looks unlikely to us.

The second model used to explain the difference between the activation energies for the conductivity and the thermoelectric power is based on small-radius polarons.[2,25] In this model, small-radius polarons are the quasiparticles which mediate the current and energy transport in a-GaSb:Ge over the entire range of germanium concentra-
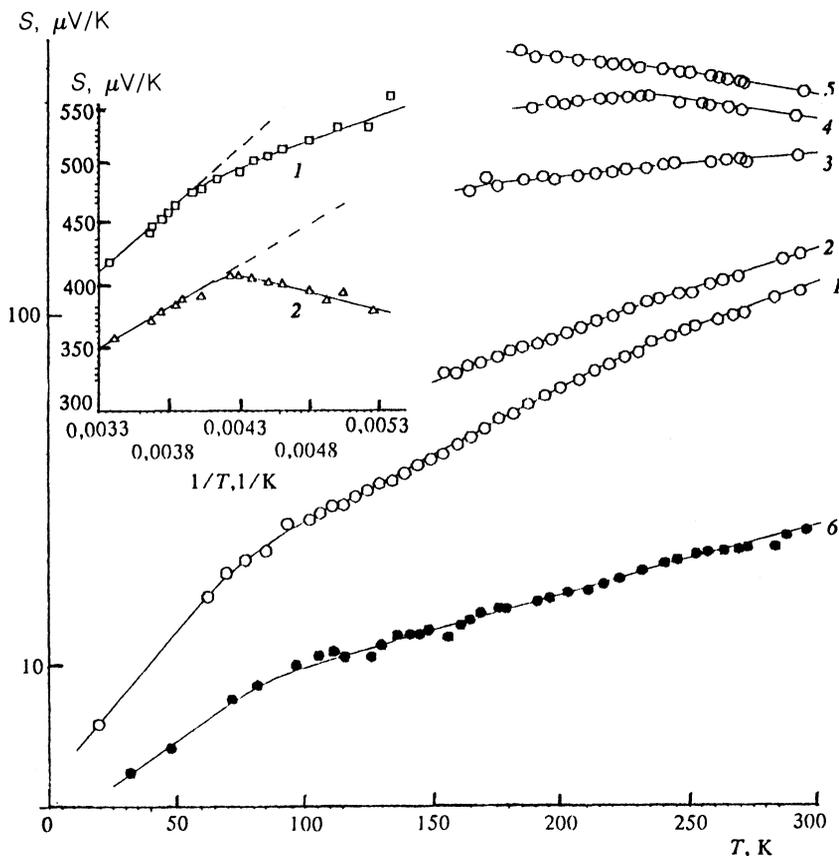
FIG. 9. Temperature dependence of the thermo-electric power of a-GaSb:Ge samples ($T_{syn}=400\,°C$). 1—$x_{Ge}=7.5$ mole %; 2—18.7; 3—30; 4—37; 5—43 mole %. Shown for comparison, by curve 6, are data on a metallic sample ($T_{syn}=1100\,°C$) with $x_{Ge}=7.5$ mole %. The $S(T)$ curves in the inset correspond to concentrations of 43 mole % (1) and 37 mole % (2).

tions. Evidence for this interpretation comes from the fact that the activation energy for the conductivity remains constant (Fig. 8b). The value of E_a in this case depends on only the average distance between atoms and the dielectric constant,[2] and the latter apparently depends only weakly on the fine details of the energy spectrum. Values close to the experimental values found for E_a (Fig. 8b) have been found for samples of the a-GaSb:Cu system.[3]

In the region $x_{Ge} \leqslant 37$ mole %, however, we have $\partial S/\partial T > 0$, and the temperature dependence of the thermoelectric power is quasimetallic (Fig. 9). One might suggest that the absence of an asymptotic behavior $S \sim E_a/T$ stems from phonon drag effects,[27] which may also be important in the case of amorphous semiconductors.[25] Unfortunately, an experimental test of that hypothesis would require extending the $S(T)$ measurements into a temperature region in which irreversible changes in the properties of the samples due to a structural relaxation and a crystallization become important. A correct combination of the phonon-drag and polaron-transport effects would appear to be an interesting theoretical problem.

It is interesting to note that the data on $E_a=f(x_{Ge})$ found from the measurements of the Seebeck coefficient can be extrapolated to the value $E_a=0$ for $x_{Ge} = x_{Ge}^*$ (Fig. 8c). One might thus suggest that the point of the structural transition corresponds to a structural feature in the kinetic characteristics of polarons analogous to the metal-insulator transition in doped semiconductors.[2] However, there has

been no detailed theoretical analysis of this possibility, to the best of our knowledge.

6. CONCLUSION

We have shown here that the amorphous semiconductors a-GaSb:Ge synthesized at high pressure exhibit several anomalies in their structural and kinetic characteristics.

A germanium doping level $x_{Ge} \leqslant 43$ mole % leads not to a decrease in the mean shortest interatomic distance, as might be expected on the basis of the chemical-compression effect,[15] but to an increase in this distance. At $x_{Ge} = x_{Ge}^* \approx 27$ mole %, the phase composition of the a-GaSb:Ge samples changes, with the result that the residual impurity of the crystalline phases c-GaSb and c-Ge disappears.

With further increase in x_{Ge}, the a-GaSb:Ge alloy remains spatially homogeneous, up to $x_{Ge} \sim 80$ mole %, in contrast with (for example) the a-GaSb:Cu system,[3] in which there is a copper solubility limit. The crystallization of the amorphous a-GaSb:Ge alloys is accompanied by a transition to a metastable crystalline solution $(GaSb)_{1-x}Ge_x$.

The change in phase composition at $x_{Ge} = x_{Ge}^*$ is also manifested by changes in the kinetic characteristics. In addition to the changes in the phase composition, variation of the sample properties is due to doping of the a-GaSb:Ge tetrahedral amorphous phase and the nonstoichiometric

Ga_ySb_{1-y} amorphous phase. In addition, the a-GaSb:Ge system demonstrates that an amorphous semiconductor synthesized under high pressure can undergo a change in conductivity type as a result of doping.

However, a joint analysis of data on the temperature dependence of the resistivity, on that of the thermal emf, and on the Hall effect shows that these results cannot be described completely satisfactorily by the existing models[1,2,25] which are ordinarily invoked to describe the properties of amorphous materials. The anomalies seen in the present study require some corresponding theoretical work.

We have shown that one of the most prominent physical effects in the amorphous semiconductor a-GaSb synthesized under pressure–the metastable superconductivity–can be described by a model which links the superconducting properties with inclusions of a nonstoichiometric amorphous phase Ga_ySb_{1-y}. When the complex structure of Ga_ySb_{1-y} is taken into account, it becomes possible to describe all the features observed in the superconducting properties of a-GaSb:Ge. Fluctuations in the parameter y over the volume of the sample and, apparently, a change in the short-range structure of the Ga_ySb_{1-y} phase at $y \approx 0.8$ are the physical causes of the characteristic features of the superconducting properties and the dispersion of these properties.

We are indebted to I. P. Zvyagin for useful discussions of certain aspects of this study and also A. G. Mil'vidskaya and G. P. Kolchina for furnishing the high-quality GaSb:Ge alloys.

[1] H. Fritzsche (editor), *Amorphous Silicon and Related Materials*, World Scientific, Singapore, 1989.

[2] N. F. Mott and E. A. Davis, *Electronic Processes in Non-Crystyalline Materials*, Oxford Univ. Press, New York, 1979.

[3] V. V. Brazhkin, S. V. Demishev, Yu. V. Kosichkin, A. G. Lyapin, N. E. Sluchanko, S. V. Frolov, and M. S. Sharambeyan, Zh. Eksp. Teor. Fiz. **101**, 1908 (1992) [Sov. Phys. JETP **74**, 1020 (1992)].

[4] T. F. Mazer, É. A. Smorgonskaya, K. D. Tséndin, and V. Kh. Shpunt, in *Abstracts, Second All-Union Conference on the Physics of Glassy Solids* (Riga, 12–15 November 1991), p. 62.

[5] J. D. Joannopoulos and G. Lucovsky (editors), *Physics of Hydrogenated Amorphous Silicon*, Springer-Verlag, New York, 1984.

[6] S. V. Demishev, Yu. V. Kosichkin, D. G. Lunts, A. G. Lyapin, N. E. Sluchanko, and M. S. Sharambeyan, Zh. Eksp. Teor. Fiz. **100**, 707 (1991) [Sov. Phys. JETP **73**, 394 (1991)].

[7] E. G. Ponyatovsky and O. I. Barkalov, Materials Science Report **8**, 147 (1992).

[8] A. G. Milnes, *Deep Impurities in Semiconductors*, Wiley, New York, 1973.

[9] I. T. Belash and E. G. Ponyatovskii, High Temp.-High Pressures **9**, 651 (1977).

[10] P. Duweg, R. H. Willens, and W. Klement, J. Appl. Phys. **31**, 1500 (1960).

[11] J. J. Hauser, Phys. Rev. B **11**, 738 (1975).

[12] A. F. Skryshevskiï, *Structural Analysis of Liquids and Amorphous Solids*, Vyssh. Shk., Moscow, 1980, p. 47.

[13] V. I. Iveronova and G. P. Revkevich, *Theory of X-Ray Scattering*, Izd MGU, Moscow, 1978, p. 129.

[14] *Chemical Handbook*, Vol. 1, Khimiya, Leningrad, 1971, p. 384.

[15] K. L. Kavanagh and G. S. Cargill, Phys. Rev. B **45**, 3323 (1992).

[16] J. E. Tibballs, S. M. Feteric, and Z. Barnea, Aust. J. Phys. **34**, 689 (1981).

[17] V. V. Brazhkin, *Effect of High Pressure on the Solidification of Metallic Melts (Pb, In, Cu, Binary Alloys of Copper)* (Author's Abstract, Candidate's Dissertation), Moscow, 1987.

[18] S. V. Demishev, Yu. V. Kosichkin, A. G. Lyapin, D. G. Lunts, and N. E. Sluchanko, Pis'ma Zh. Eksp. Teor. Fiz. **56**, 44 (1992) [JETP Lett. **56**, 45 (1992)].

[19] A. A. Abrikosov, *Fundamentals of the Theory of Metals*, Elsevier, New York, 1988.

[20] B. G. Lazarev, E. E. Semenkov, and V. I. Tutov, Vopr. At. Nauki Tekh. Ser. Fund. Prikl. Sverkhprovod., No. 1(4), 3 (1976).

[21] D. B. McWhan, G. W. Hull, T. R. R. McDonald, and E. Gregory, Science **147**, 1441 (1965).

[22] T. R. R. McDonald, E. Gregory, and G. S. Barberich, Phys. Lett. **14**, 16 (1965).

[23] A. S. Skal, Zh. Eksp. Teor. Fiz. **88**, 516 (1985) [Sov. Phys. JETP **61**, 302 (1985)].

[24] B. I. Shklovskiï, Zh. Eksp. Teor. Fiz. **72**, 288 (1977) [Sov. Phys. JETP **45**, 152 (1977)].

[25] I. P. Zvyagin, *Kinetic Phenomena in Disordered Semiconductors*, Izd MGU, Moscow, 1984, p. 160.

[26] Y. P. Varshni, Physica **34**, 149 (1967).

[27] K. Seeger, *Semiconductor Physics*, Springer-Verlag, New York, 1974.

Translated by D. Parsons